Available online at www.derpharmachemica.com

ISSN 0975-413X
CODEN (USA): PCHHAX

Der Pharma Chemica, 2016, 8(12):36-44
(http://derpharmachemica.com/archive.html)

Synthesis, Characterization, Crystal structure and Hirshfeld Surface Analysis of (2-oxo-2H-pyridin-1-yl)-acetic acid hydrazide

Zabiulla[1#], S. Naveen[2#], S. V. Mamatha[1], Mahima Jyothi[1], N. S. Lingegowda[3], N. K. Lokanath[4] and Shaukath Ara Khanum[1*]

[1]*Department of Chemistry, Yuvaraja's College, University of Mysore, Mysuru 570 005, India*
[2]*Institution of Excellence, Vijnana Bhavana, Manasagangotri, University of Mysore, Mysuru 570 006, India*
[3]*Department of Chemistry, Vidyavardhaka College of Engineering, Visvesvaraya Technological University, Mysuru 570 002, India*
[4]*Department of Studies in Physics, Manasagangotri, University of Mysore, Mysuru 570 006, India*

ABSTRACT

The title compound, (2-oxo-2H-pyridin-1-yl)-acetic acid hydrazide was synthesized in good yield by refluxing 2-hydroxypyridine with ethyl chloroacetate in the presence of K_2CO_3 in anhydrous acetone. The product obtained was characterized by spectroscopic techniques and finally the structure was confirmed by X-ray diffraction studies. The compound crystallizes in the monoclinic crystal system with the space group $P2_1/c$ with unit cell parameters a = 8.6789(4) Å, b = 10.4374(5) Å, c = 8.3596(4) Å, β = 92.873(3)° and Z=4. The crystal structure features two strong N--H…O hydrogen bonds with different packing motifs. Hirshfeld surface analysis for visually analyzing intermolecular interactions in crystal structures employing molecular surface contours and 2D fingerprint plots have been used to examine molecular shapes.

Keywords: 2-Hydroxy pyridine, Crystal structure, Dimeric chain, Hirshfeld Surfaces, N--H...O and C--H…O interactions.

INTRODUCTION

Pyridine is one of the most prevalent heterocyclic compounds in nature. It is present in natural compounds like nicotinic acid (vitamin B3) and pyridoxine (vitamin B6) and in numerous alkaloids. Further it plays a central role as versatile building block in the synthesis of natural products as well as biologically active compounds. Also, pyridine bases are widely used in pharmaceutics as nicotinamides and nicotinic acid derivatives. The various therapeutic potential of pyridine derivatives have been reported in the treatment of cancers of diverse cells, by targeting angiogenesis [1,2], apoptosis [3, 4] and by inhibiting wide range of tumour promoting factors like, FAK [5], CDK [3-6] and topoisomerase **II** [7] and also antiproliferative and apoptogenic properties against Dalton's lymphoma was repoted [8]. Many Hydrazides derivatives display diverse pharmacological activities such as anti-inflammatory [9], antidiabetic [10], anticancer [11], antitumour and analgesic activities [12]. Isoniazid (isonicotinohydrazide) is an antituberculosis drug [13], while Iproniazid (N'-isopropylisonicotinohydrazide) possesses antidepressant activity [14]. Phenelzine ((2-phenylethyl) hydrazine) is a good chemical to be used as muscle relaxant. Similarly, Hydralazine is used to treat hypertension [15]. Sulfonylhydrazide derivatives act as DNA modifying agents and have antitumor activities against murine tumors, including the B16 melanoma, M109 lung carcinoma, L1210 leukemias, P388 and M5076 reticulum cell sarcoma [11]. In view of their broad spectrum of biological properties and as a part of our ongoing work on synthesis and characterization of novel compounds [16,17], the title compound was synthesized. The compound obtained was characterized spectroscopically and finally the structure was confirmed by X-ray diffraction studies. An investigation of close intermolecular contacts between the molecules *via* Hirshfeld surface analysis is also presented in order to quantify the interactions within the crystal structure.

MATERIALS AND METHODS

All the chemicals were purchased from Sigma Aldrich Chemical Co. ^{1}H NMR spectra was recorded on a Bruker 400 MHz in $CDCl_3$ and the chemical shifts were recorded in parts per million downfield from tetramethylsilane. Mass spectra were obtained with a VG70-70H spectrophotometer. The elemental analysis of the compounds was performed on a Perkin Elmer 2400 Elemental Analyzer. The results of elemental analyses were within ±0.4% of the theoretical values.

Synthesis of(Pyridin-2-yloxy)-acetic acid ethyl ester 2:
A mixture of 2-hydroxy pyridine (**1**, 0.03 mol) and ethyl chloro acetate (**2**, 0.045 mol) in dry acetone (40 ml) was treated with anhydrous potassium carbonate (6.2 g, 0.045 mol) and refluxed for 12 h. The reaction mixture was cooled and solvent removed by distillation. The residual mass was triturated with cold water to remove potassium carbonate, and extracted with ether (3×30 ml). The ether layer was washed with 10% sodium hydroxide solution (3×30 ml) followed by water (3×30 ml) and then dried over anhydrous sodium sulphate and evaporated to afford compound 2 as a yellow liquid [18, 19].

Yield 88%; IR (cm^{-1}): 1740 (C=O); ^{1}H NMR (DMSO-d_6): δ 2.5 (t, 3H, CH_3 of ester), 3.8 (q, CH_2 of ester), 4.5 (s, 2H, CH_2), 6.6-7.8 (m, 4H, pyridine Ar-H); LC-MS m/z 182 (M+1); Anal. Cal. for $C_9H_{11}NO_3$ (181): C, 59.66; H, 6.12; N, 7.73. Found: C, 59.46; H, 6.34; N, 7.49%.

Synthesis of (Pyridin-2-yloxy)-acetic acid hydrazide 3:
Compound (**3**, 2.6 g, 0.01 mol) was dissolved in ethanol (20 ml). Hydrazine hydrate (1.4 g, 0.035 mol) was added to this and the mixture was stirred for 6 hrs. The precipitate was filtered, washed with water to get compound 3 as a white solid.

Yield 75%. M.P. 115-117 ^{o}C. IR (KBr, cm^{-1}): 1670 (amide, C=O), 3120-3220 (NH-NH_2). ^{1}H NMR (DMSO-d_6): δ: 4.5 (s, 2H, CH_2), 6.5-7.7 (m, 4H, pyridine Ar-H), 12.3 (s, 1H, NH). LC-MS m/z 168 (M+1).Anal. Cal. for $C_7H_9N_3O_2$ (167): C, 50.29; H, 5.43; N, 25.14. Found: C, 50.21; H, 5.41; N, 25.08%.

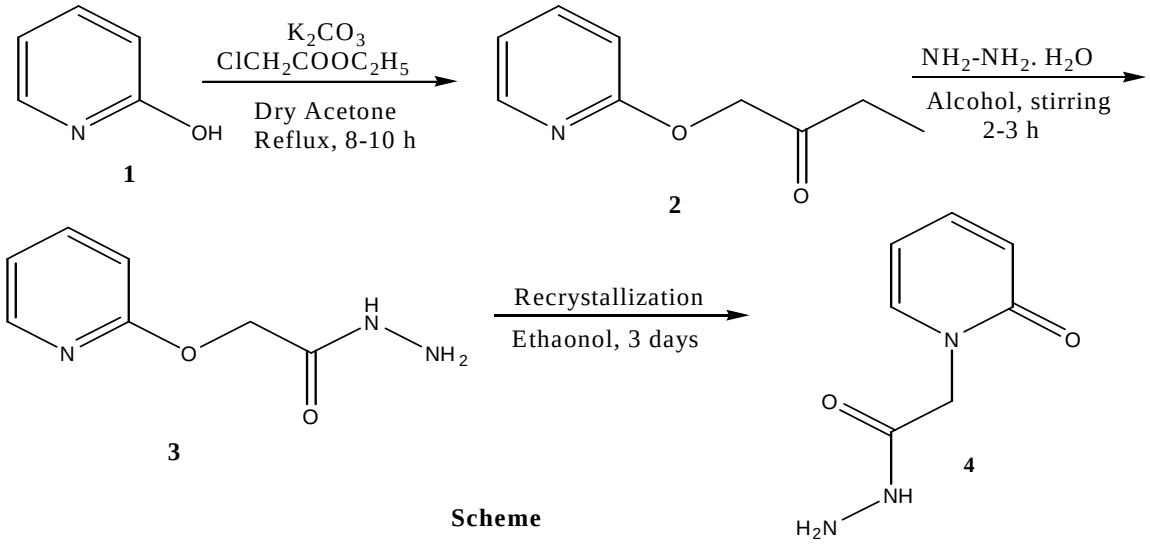

Scheme 1: Synthesis of (2-oxo-2H-pyridin-1-yl)-acetic acid hydrazide

Synthesis of (2-oxo-2H-pyridin-1-yl)-acetic acid hydrazide 4:
Compound (**3**) in ethanol (10 ml) was kept for crystallization for 3 days and was left undisturbed at room temperature to obtain white crystals of (2-oxo-2H-pyridin-1-yl)-acetic acid hydrazide (**4**). A schemtaic diagram of the synthesized molecule is shown in scheme 1.

Yield 75%. M.P. 142-144 ^{o}C. IR (KBr, cm^{-1}): 1675 (amide, C=O), 3130-3230 (NH-NH_2). ^{1}H NMR (DMSO-d_6): δ:4.0 (s, 1H, NH_2), 4.4 (s, 2H, CH_2), 6.6-7.8 (m, 4H, pyridine Ar-H), 9.7 (s, 1H, NH). LC-MS m/z 168 (M+1); Anal. Cal. for $C_7H_9N_3O_2$ (167): C, 50.29; H, 5.43; N, 25.14. Found: C, 50.25; H, 5.39; N, 25.09%.

2.2 Crystal Structure Determination
A white coloured rectangle shaped single crystal of dimensions 0.29×0.27×0.22 mm of the title compound was

chosen for an X-ray diffraction study. The X-ray intensity data were collected at a temperature of 296 K on a Bruker Proteum2 CCD diffractometer equipped with an X-ray generator operating at 45 kV and 10 mA, using CuK_{α} radiation of wavelength 1.54178 Å.Data were collected for 24 frames per set with different settings of φ(0° and 90°), keeping the scan width of 0.5°, exposure time of 2 s, the sample to detector distance of 45.10 mm and 2θvalue at 46.6°. A complete data set was processed using *SAINT PLUS* [20]. The structure was solved by direct methods and refined by full-matrix least squares method on F^2 using *SHELXS* and *SHELXL* programs [21]. All the non-hydrogen atoms were revealed in the first difference Fourier map itself.All the hydrogen atoms were positioned geometrically (C–H = 0.93Å, O–H = 0.82 Å) and refined using a riding model with U_{iso}(H) = 1.2 $U_{eq}$and 1.5 U_{eq}(O). After several cycles of refinement, the final difference Fourier map showed peaks of no chemical significance and the residuals saturated to 0.0345. The geometrical calculations were carried out using the program *PLATON* [22].The molecular and packing diagrams were generated using the software *MERCURY* [23]. The details of the crystal structure and data refinement are given in **Table 1**. **Figure 1** represents the ORTEP of the molecule with thermal ellipsoids drawn at 50% probability.

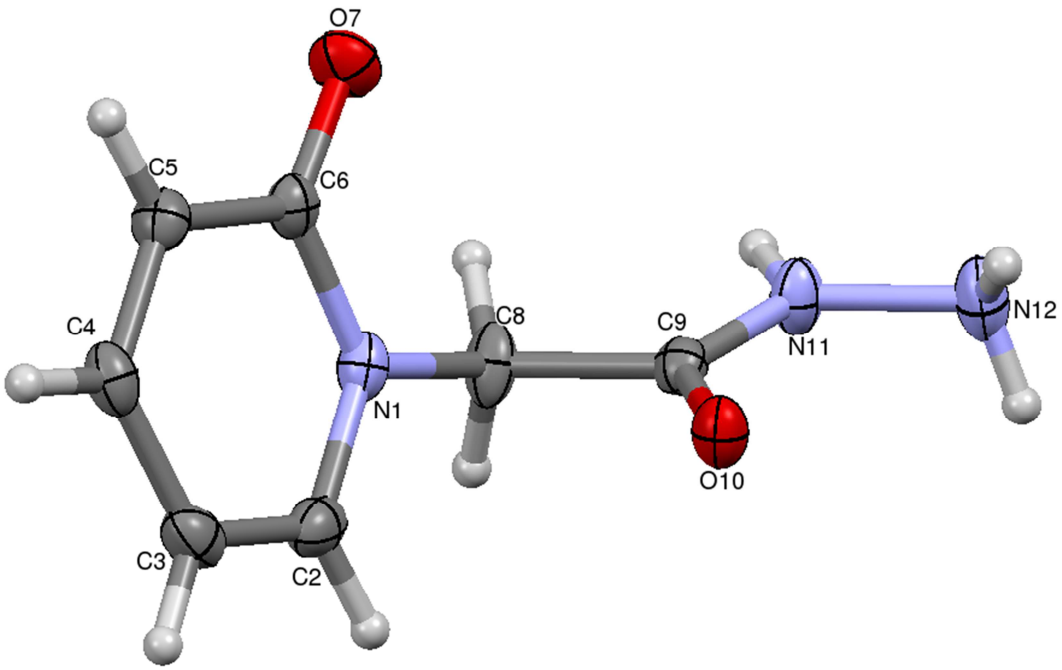

Figure 1: ORTEP of the molecule with thermal ellipsoids drawn at 50% probability

Table 1: Crystal data and structure refinement table

Parameter	Value
CCDC deposit No.	CCDC 1488797
Empirical formula	$C_7H_9N_3O_2$
Formula weight	167.17
Temperature	293(2) K
Wavelength	1.54178 Å
Crystal system, space group	Monoclinic, $P2_1/c$
Unit cell dimensions	a = 8.6789(4) Å b = 10.4374(5) Å c = 8.3596(4)Å β = 92.873(3)º
Volume	756.30(6) $Å^3$
Z, Calculated density	4, 1.468 Mg/m^3
Absorption coefficient	0.932 mm^{-1}
$F_{(000)}$	352
Crystal size	0.29 x 0.27 x 0.22 mm
Theta range for data collection	5.10º to 64.37°
Limiting indices	-10≤ h ≤ 9, -12 ≤ k ≤ 12, -9 ≤ l ≤ 9
Reflections collected / unique	4848/ 1224 [R(int) = 0.0367]
Refinement method	Full-matrix least-squares on F^2
Data / restraints / parameters	1224 / 0 / 110
Goodness-of-fit on F^2	1.059
Final R indices [$I>2\sigma(I)$]	$R1$ = 0.0345, $wR2$ = 0.0901
R indices (all data)	$R1$ = 0.0388, $wR2$ = 0.0927
Largest diff. peak and hole	0.189 and −0.191 e. $Å^{-3}$

Hirshfeld surface calculations

Molecular Hirshfeld surface in the crystal structure was created based on the electron distribution calculated as the sum of spherical atom electron densities. The normalized contact distance (d_{norm}) based on both d_e, $d_i$and the *van Der Waals radii* of the enables identification of the regions of particular importance to intermolecular interactions. The Hirshfeld surfaces and fingerprint plots presented here were plotted using the software CrystalExplorer 3.0 [24]. The d_{norm} plots were mapped with colour scale in between −0.18 au (blue) and 1.4 au (red). The 2D fingerprint plots [25, 26] were displayed by using the expanded 0.6–2.8 Å view with the d_e and d_i distance scales displayed on the graph axes. When the cif file was uploaded into the CrystalExplorer software, all bond lengths to hydrogen were automatically modified to typical standard neutron values i.e., C–H = 1.083Å.

RESULTS AND DISCUSSION

The pyridine ring is planar. The pendant acetic acid hydrazide is in an extended conformation and makes a dihedral angle of 72.95(1)° from the plane of the pyridine ring. This value is slightly higher than the reported value of 67.57(1)° for 2,6-difluoro phenoxy acetic acid [27]. The structure exhibits both inter and intramolecular hydrogen bonds of the type N--H...O and C--H...O. The crystal structure features two strong N--H…O hydrogen bonds with different packing motifs. Of the two, one (N11--H11…O7) is involved in forming a dimeric $R^2_2(14)$ ring (**Figure 2**), while, the other (N12--H12A…O7)connects these dimeric units into *C(8)* chains, and thus a two dimensional network is observed. The adjacent two dimensional networks are interconnected by C-H…O interactions forming a 3D architecture. The crystal packing is further stabilized by *pi…pi* interactions (Cg...Cg = 3.4870Å)(**Figure 3**).

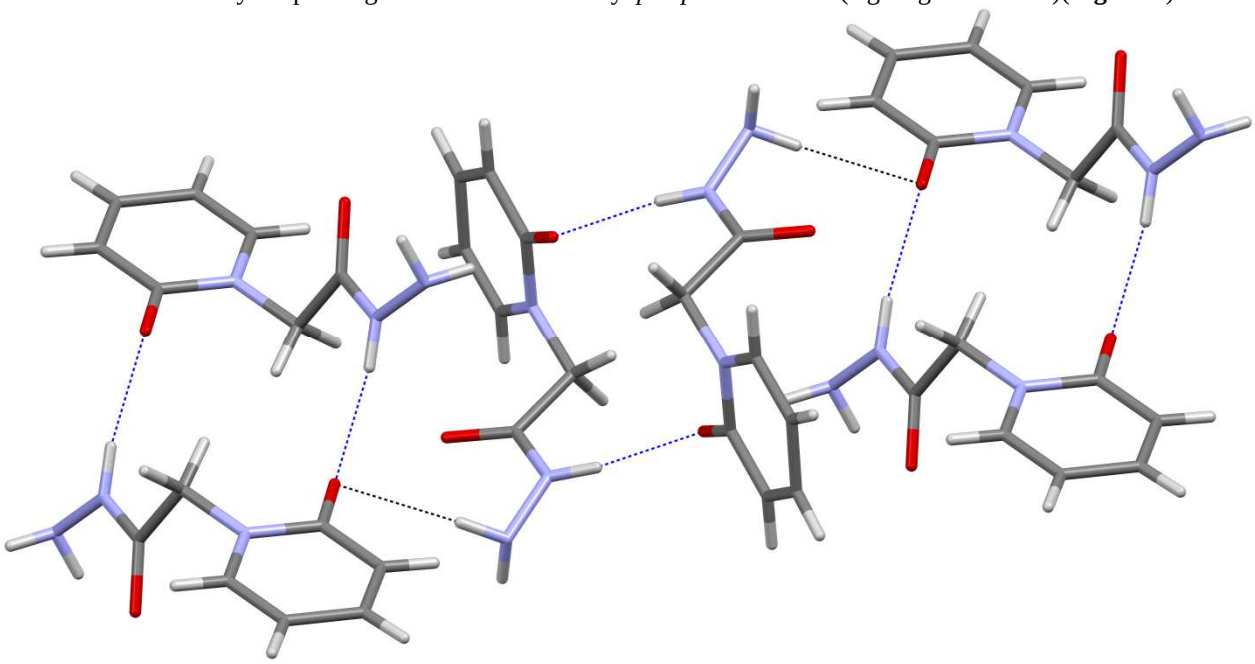

Figure 2: Packing of the molecules showing the dimeric $R^2_2(14)$ ring. The dotted lines represent the N11--H11…O7 intermolecular hydrogen bonds

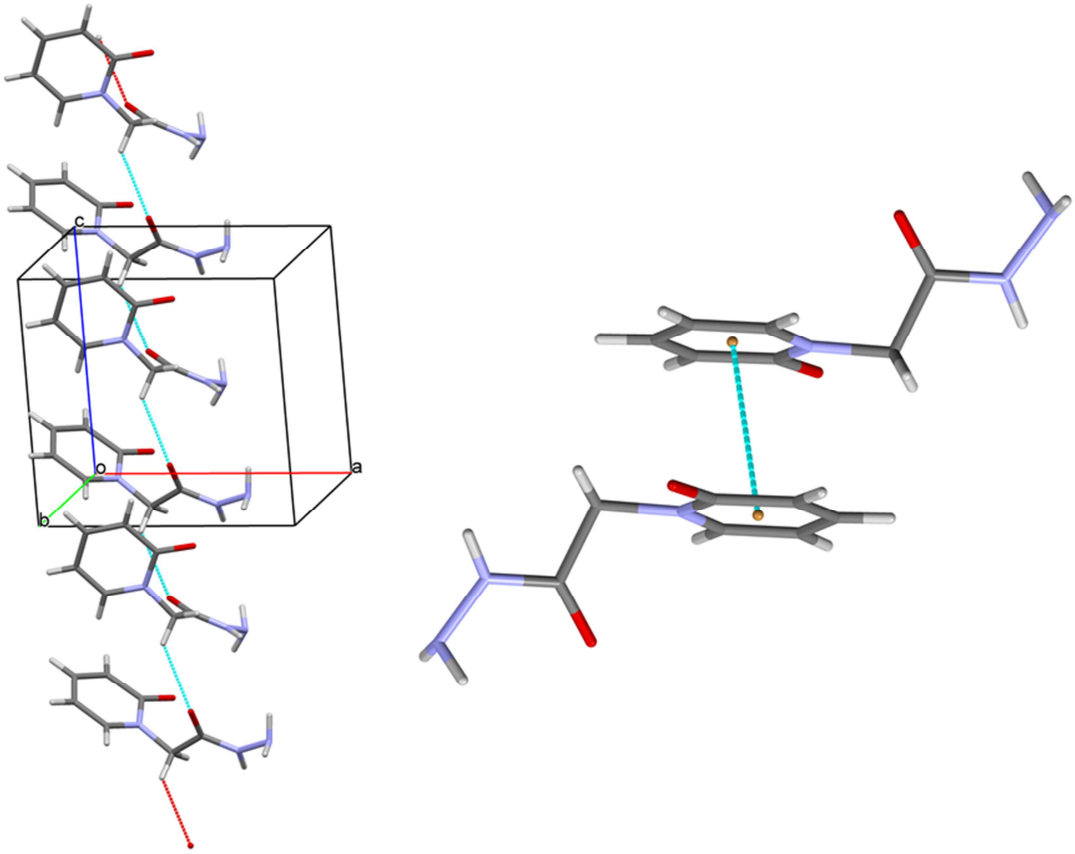

Figure 3: Packing of the molecules when viewed along the *b* axis. The dotted lines represent intermolecular hydrogen bond N12--H12A…O7 forming *C(8)* chains

Hirshfeld surface studies

Hirshfeld surface analysis is an effective tool for exploring packing modes and intermolecular interactions in molecular crystals, as they provide a visual picture of intermolecular interactions and of molecular shapes in a crystalline environment. Surface features characteristic of different types of intermolecular interactions can be identified, and these features can be revealed by colour coding distances from the surface to the nearest atom exterior (d_e plots) or interior (d_i plots) to the surface. This gives a visual picture of different types of interactions present and also reflect their relative contributions from molecule to molecule. Further, 2D fingerprint plots (FP), in particular the breakdown of FP into specific atom…atom contacts in a crystal, provide a quantitative idea of the types of intermolecular contacts experienced by molecules in the bulk and presents this information in a convenient colour plot. Hirshfeld surfaces comprising d_{norm} surface and Finger Print plots were generated and analysed for the title compound in order to explore the packing modes and intermolecular interactions. The two dimensional fingerprint plots from Hirshfeld surface analyses **Figure 4**,illustrates the difference between the intermolecular interaction patterns and the relative contributions to the Hirshfeld surface (in percentage) for the major intermolecular contacts associated with the title compound. The fingerprint plots can be decomposed to highlight particular atoms pair close contacts. There are two sharp spikes pointing toward the lower left of the plots and are typical C—H…O hydrogen bonds. Importantly, H...H (42%) bonding appears to be a major contributor in the crystal packing, whereas the O...H/H...O (29.3%), C...H/H...C (14.12%), N...H/H...N(6.7%) plots also reveal the information regarding the intermolecular hydrogen bonds thus supporting for the N--H...Oand C--H...O interactions.

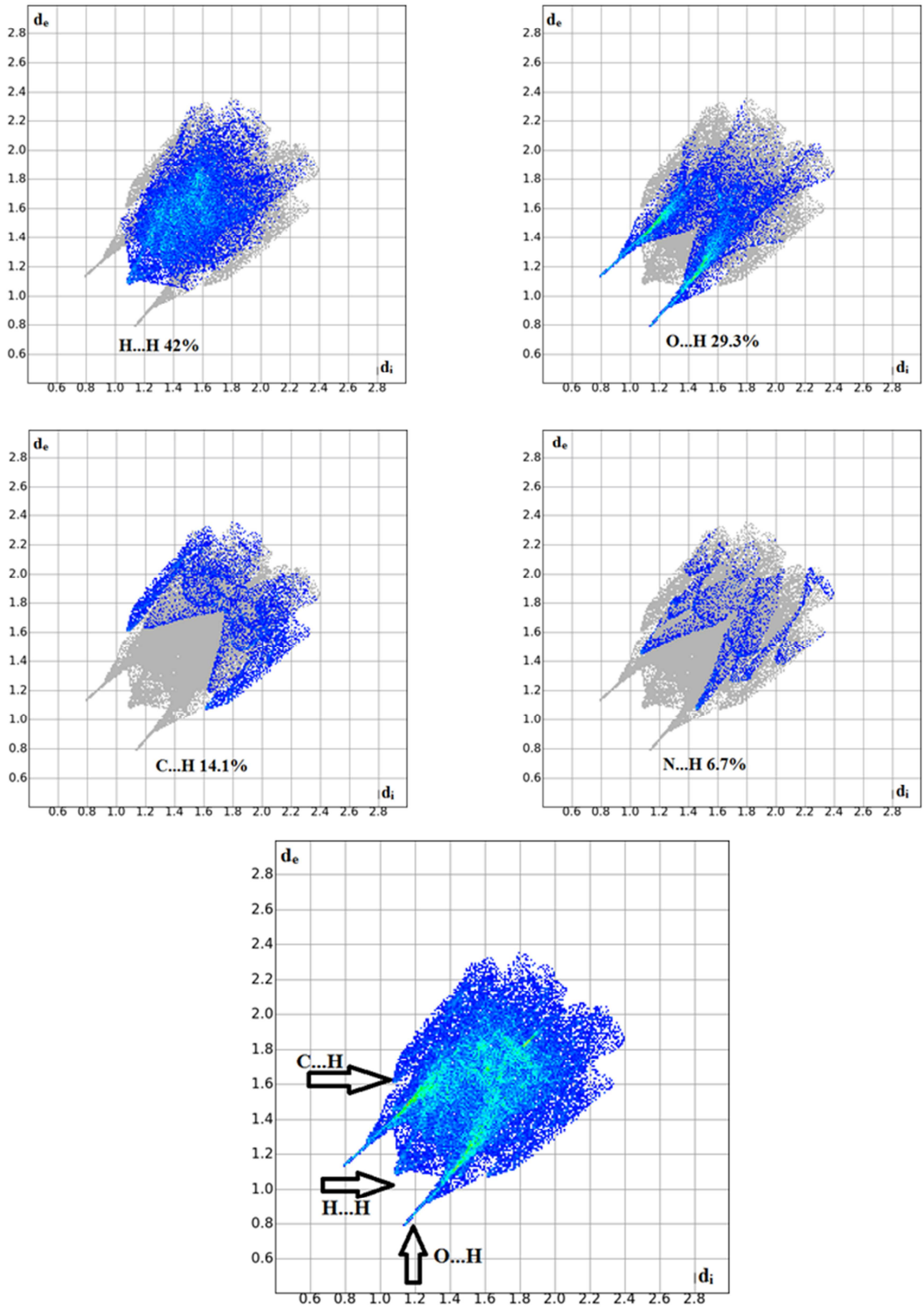

Figure 4: Fingerprint plots of the title compound showing H...H, O…H,C...H and N...H interactions. d_i is the closest internal distance from a given point on the Hirshfeld surface and d_e is the closest external contacts

This intermolecular contact is highlighted by conventional mapping of d_{norm} on molecular Hirshfeld surfaces and is shown in **Figure 5**. The red spots over the surface indicate the intercontacts involved in hydrogen bond. The dark-red spots on the d_{norm} surface arise as a result of the short interatomic contacts, i.e., strong hydrogen bonds, while the other intermolecular interactions appear as light-red spots.

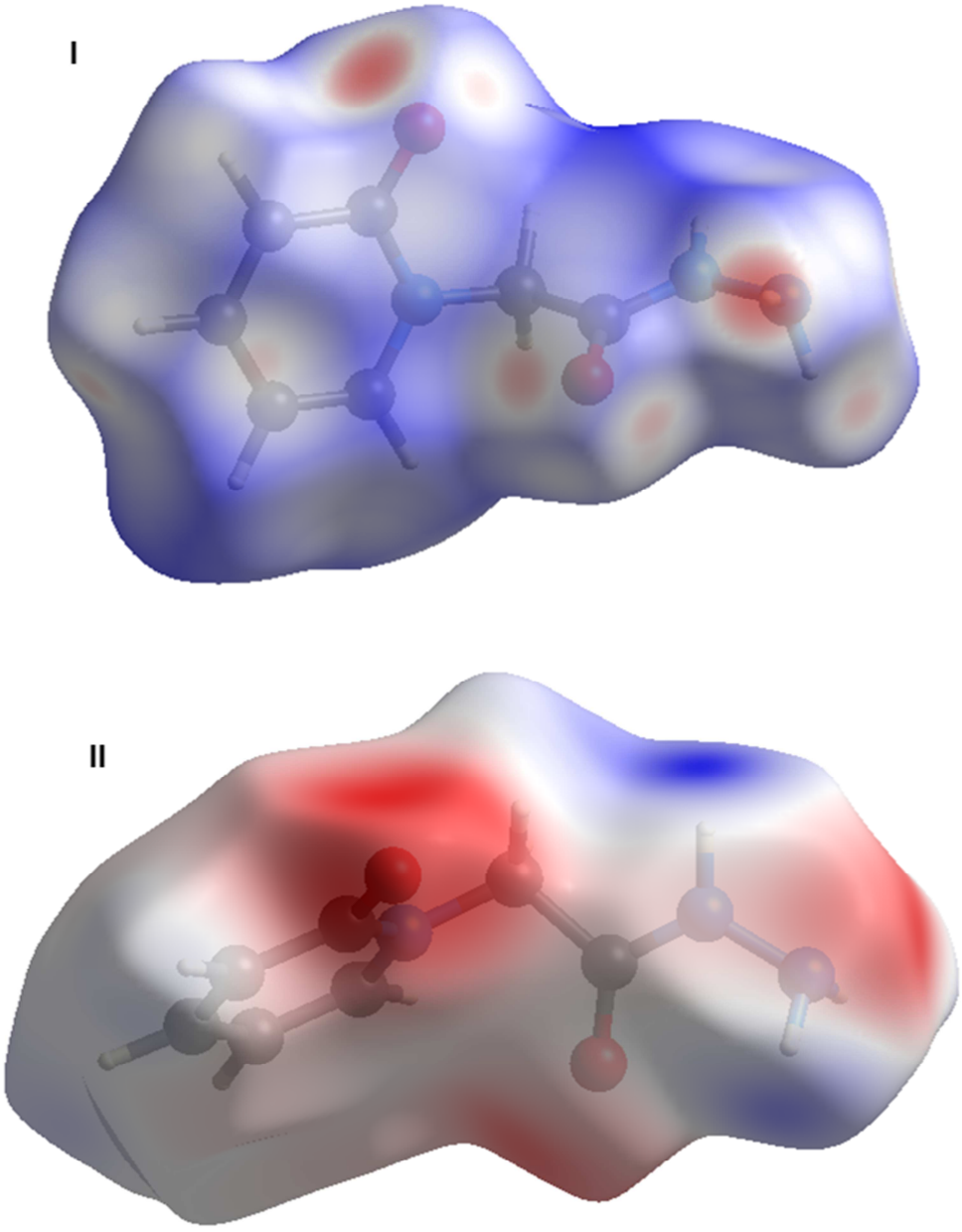

Figure 5:d_{norm}(I) and electrostatic potential(II) mapped on Hirshfeld surface for visualizing the intermolecular contacts

Figure 6 shows the shape index and curvedness mapped on Hirshfeld surface indicating the largest regions of flat curvedness appearing for the title compound. The shape index surface clearly shows that the two sides of the molecules are involved in same contacts with neighbouring molecules and curvedness plots show flat surface patches characteristic of planar stacking.

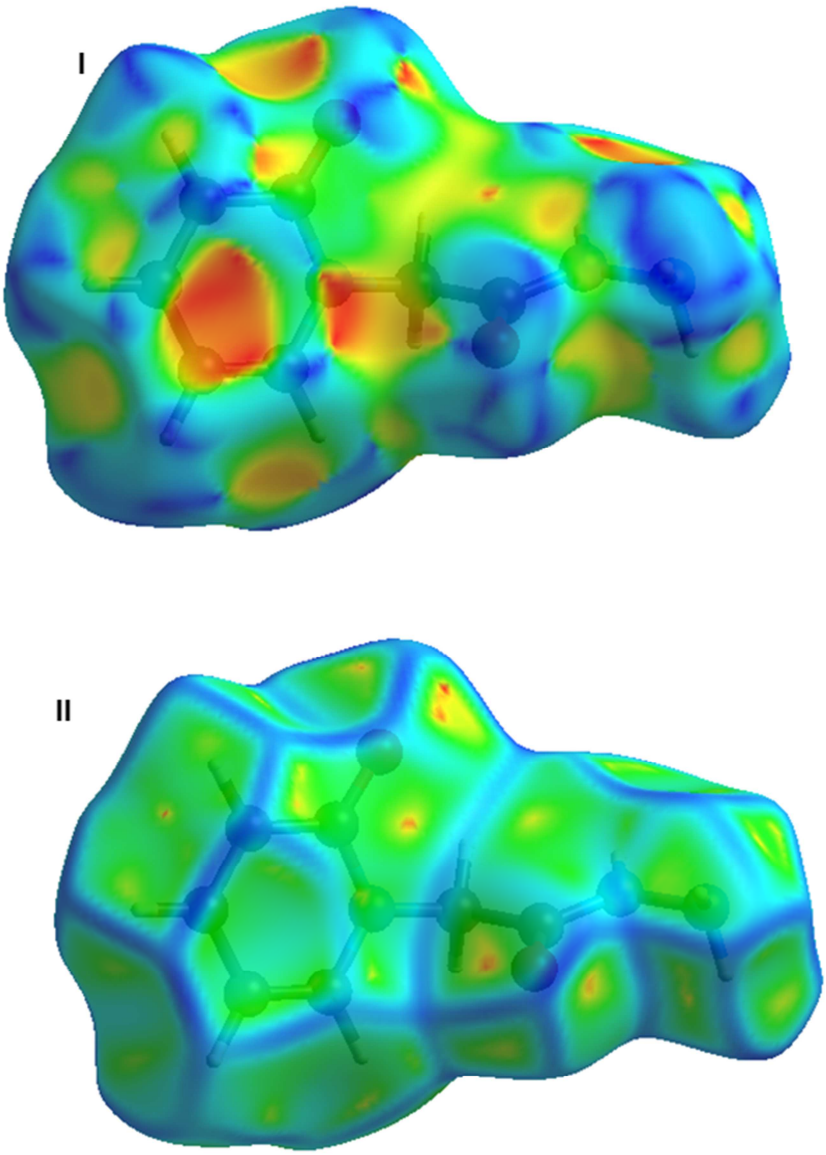

Figure 5: Shape index(I) and curvedness index(II) mapped on the Hirshfeld surface. The surfaces are shown as transparent to allow visualization of the orientation and conformation of the functional groups in the molecules

Acknowledgments

The authors are grateful to the Institution of Excellence, Vijnana Bhavana, University of Mysore, India, for providing the single-crystal X-ray diffractometer facility. Zabiulla gratefully acknowledges the financial support provided by the Department of Science and Technology, New Delhi, Under INSPIRE-Fellowship scheme [IF140407]. Shaukath Ara Khanum thankfully acknowledges the financial support provided by VGST, Bangalore, under CISEE Programme [Project sanction order: No. VGST/ CISEE /282].

REFERENCES

[1] P. M. Lukasik, S. Elabar, F. Lam, H. Shao, X. Liu, A. Y. Abbas, and S. Wang, *Eur. J. Med. Chem.* **2012,** 57, 311–322.
[2] C. M. Ahn, W. S. Shin, H. Bum Woo, S. Lee, and H. W. Lee, *Bioorg. Med. Chem. Lett.***2014,** 15, 3893–3896.
[3]F. Ari, N. Aztopal, C. Icsel, V. T. Yilmaz, E. Guney, O. Buyukgungor, and E. Ulukaya, *Bioorg. Med. Chem.*,**2013,** 21(21), 6427–6434.
[4] Y. B. Zhang, W. Liu, Y. S. Yang, X. L. Wang, H. L. Zhu, L. F. Bai, and X. Y. Qiu, *Med. Chem. Res.*, **2013,** 22, 3193–3203.
[5]U. R. Chamakura, E. Sailaja, B. Dulla, A. M. Kalle, S. Bhavani, D. Rambabu, R. Kapavarapu, M. V.

BasaveswaraRao, and M. Pal, *Bioorg. Med. Chem. Lett.*,**2014,** 24, 1366–1372.
[6] R. Karki, C. Park, K. Y. Jun, J. G. Jee, J. H. Lee, P. Thapa, T. M. Kadayat, Y. Kwon, and E. S. Lee, *Eur. J. Med. Chem.*, **2014,** 84, 555–565.
[7] J. A. Varela, and C. Sáa, *Chem. Rev.*, **2003,**103, 3787–3802.
[8] Mohammed Al-Ghorbani ,PrabhuThirusangu, H. D. Gurupadaswamy, V. Girish, H. G. ShamanthNeralagundi, B. T. Prabhakar and ShaukathAraKhanum, *Bioorg. Chem.*, **2016,** 65,73–81.
[9] A. Ignat, V. Zahari, C. Mogos¸ N. Palibroda, C. Cristea, and L. S. Dumitrescu, *Farmacia*, **2010,** 3, 290-302.
[10] S. Tyagi, S. Kumar, A. Kumar, and M. Singla, *Int. J. PharmaWorld Res.*,**2010,** 1, 1-16.
[11] R. A. Finch, K. Shyam, P. G. Penketh and A. C. Sartorelli, *Cancer Res.*,**2001**, 61, 3033-3038.
[12] L. L. Silva, K. N. Oliveira, and R. J. Nunes, *ARKIVOC* **2006,** 13, 124-129.
[13] P. Ahmed, M. Anwar, B. Khan, C. Altaf, K. Ullah, S. Raza, and I. Hussain, *J. Pak. Med. Assoc.* **2005**, 55, 378-381.
[14] E. D. West, and P. G. Dally, *Brit. Med. J.*, **1959**, 5136, 1481-1482.
[15] A. Nazir, J. Sadaf, and S. Saleem, *J. Surg. Pak.*, **2011**, 71-74.
[16] B. Dinesh, H. R. Manjunath, S. Naveen, K. Abhiraj, A. Ramesha Baba, D. Channe Gowda, M. A. Sridhar, and J. Shashidhara Prasad, *Mol. Cryst. Liq. Cryst.*, **2010,** 517,161-166.
[17] P. S. Pradeep, S. Naveen, M. N. Kumara, K. N. Mahadevan, and N. K. Lokanath, **2014,** E70, 153-156.
[18] S. A. Khanum, S. Shashikanth, and A. V. Deepak, *Bioorg. Chem.*,**2004**, 32, 211–222.
[19] M. Ahmed, R. Sharma, D. P. Nagda, J. L. Jat, and G. L. Talesara, *Arkivoc*, **2006**, XI, 66–75.
[20] Bruker, **2004**, APEX2, SAINT-Plus and SADABS. Bruker AXS Inc., Madison, Wisconsin, USA.
[21] G. M. Sheldrick, *ActaCryst*.,**2015**, A71, 3-8.
[22] A. L. Spek, *Acta. Cryst*.,**1990**, A46, C34-C37.
[23] C. F. Macrae, I. J. Bruno, J. A. Chisholm, P. R. Edgington, P. McCabe, E. Pidcock, L. Rodriguez-Monge, R. Taylor, J. van de Streek, P. A. Wood, *J. Appl. Cryst*., **2008**, 41, 466.
[24] S. K. Wolff, D. J. Grimwood, J. J. McKinnon, D. Jayatilaka, M. A. Spackman, Crystal Explorer 3.0, University of Western Australia, Perth, Australia, **2001**.
[25] K. S. Saikat, *CrystEng Comm*., **2013**, 9, 1772-1781.
[26] K. S. Saikat, *J. Mol. Struct.*, **2014**, 1064, 70-75.
[27] Y. H. I. Mohammed, S. Naveen, H. H. Issa, H. R. Manjunath, N. K. Lokanath and S. A. Khanum, *Der PharmaChemica*, **2016**, 8(2), 286-291.